AAEC/E382

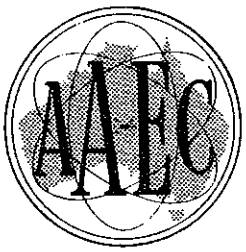

AAEC/E382

AUSTRALIAN ATOMIC ENERGY COMMISSION

RESEARCH ESTABLISHMENT

LUCAS HEIGHTS

TRANSVERSE CRACKING IN ORTHOTROPIC GLASS FIBRE / EPOXY RESIN COMPOSITES

by

G.T. STEVENS
A.W. LUPTON

October 1976
ISBN 0 642 99732 2

AUSTRALIAN ATOMIC ENERGY COMMISSION
RESEARCH ESTABLISHMENT
LUCAS HEIGHTS

TRANSVERSE CRACKING IN ORTHOTROPIC GLASS FIBRE/EPOXY RESIN COMPOSITES

by

G.T. STEVENS
A.W. LUPTON

ABSTRACT

The transverse cracking in glass-fibre composites based on (i) an unmodified epoxy resin system, (ii) a flexibilised epoxy system and (iii) an epoxy containing an elastomeric toughening agent, was studied under direct tensile loading and repeated tensile loading at room temperature, 75°C and 100°C.

It was found that when the resin is in the glassy state, the final crack spacing and the relationship between stress and crack spacing can be explained in terms of shear stress transfer from the longitudinal plies. If the toughness of the resin is sufficient to allow slow crack growth, a more closely spaced array of irregular cracks is formed. The elastic modulus of the laminate is lowered by transverse cracking, but the modulus in both the cracked and uncracked state is not greatly affected by the modulus of the resin. The high ductility of the resins in the rubbery state is not sufficient to prevent transverse cracking although, because of the very low modulus of the resin in this state, such cracking is not accompanied by large reductions in the stiffness of the laminate.

National Library of Australia card number and ISBN 0 642 99732 2

The following descriptors have been selected from the INIS Thesaurus to describe the subject content of this report for information retrieval purposes. For further details please refer to IAEA-INIS-12(INIS: Manual for Indexing) and IAEA-INIS-13 (INIS: Thesaurus) published in Vienna by the International Atomic Energy Agency.

COMPOSITE MATERIALS; CRACKING; DUCTILITY; ELASTICITY; EPOXIDES; FIBERS; GLASS; MEDIUM TEMPERATURE; RESINS

CONTENTS

CONTENTS (Continued)

1. INTRODUCTION

When strands of glass fibres are aligned and bound with a suitable resin, a low cost composite with a high strength to weight ratio is formed. A major disadvantage of this material is its high anisotropy; the high strength properties are confined to the direction of the fibres, and the strength and modulus are quite low at substantial deviations from that direction.

In most applications, strength and stiffness are required in more than one direction and the fibres must be arranged accordingly. The most efficient method is to form layers (plies) of unidirectionally aligned fibres into a laminate in which the different plies have their fibres aligned in the optimum directions. This arrangement is not without its disadvantages, however, because although the ply containing the fibres in the direction of the load may withstand the imposed load, the other plies may actually fail. The failure takes the form of cracking in the resin between the fibres with cracks running more or less across the thickness of the ply and parallel to the axis of the fibres. Although the laminate is still intact, the stiffness is decreased and the permeability increased with the result that the component may be unsuitable for further service.

This report describes the initial stages of a project aimed at alleviating transverse cracking in glass fibre/epoxy resin composites and modifying a practical epoxy resin system to give substantial cracking resistance to composites at temperatures around 70°C.

2. BACKGROUND

The phenomenon of transverse cracking (also termed 'crazing') first received serious attention during the development of composite pressure vessels for the United States' guided missile program.

Rawe [1962] found that cracking in filament-wound vessels was related to voids or resin-rich areas in the laminate; he suggested that the efforts to eliminate cracking should be directed to more accurate fibre placement and improvements in resin toughness. His suggestions were supported in the theoretical papers of Kies [1962] and Schultz [1963]; they identified the cause as the strain concentration effects

of the fibres. Because the fibres are much stronger and stiffer than the resin, most of the transverse strain must be borne by the thin layer of resin between the fibres. In a typical laminate with regular fibre spacing, a strain magnification of about ten is predicted.

Epstein & Bandaruk [1964] noted that with a resin which had a failure strain of about 3 per cent, cracking occurred at a composite strain in the range 0.3 to 0.4 per cent; this agreed with the above theoretical analyses. In their study of pressure vessels they made the following points:

(i) The cracking is associated with debonding at or adjacent to the resin glass interface.

(ii) A discontinuity ('knee') occurs in the stress strain curve as a result of cracking (Figure 1).

(iii) Cracking results in permanent dimensional changes.

(iv) Increasing the resin ductility increases the resistance to cracking.

Since these analyses, the cracking of vessels has received little attention. The problem appears not to have been solved but rather avoided, either by the use of a flexible liner to prevent fluid penetration or by resorting to higher modulus (and higher priced) fibres in which the overall strain of the composite is restricted.

Increasing the ductility of the resin appears to be an obvious way in which to eliminate cracking. Lavengood & Ishai [1971] have shown explicitly, in specimens cut from flat orthotropic sheet, that increasing the ductility results in an increase in the strain necessary for cracking.

The ductility of epoxy resins is generally increased by incorporating long chain elements (flexibiliser) into the cross-linked structure to force the molecules apart and thus facilitate movement of the structure under stress. However, thermal movements are also assisted and the glass transition temperature (the temperature above which the resin is no longer glassy but rubbery) is lowered.

McGarry & Willner [1968] showed that epoxy resins could be considerably toughened by the introduction of discrete particles of an elastomer which bonds to the resin (a process that is effectively used to toughen thermoplastic materials); this toughening process has been developed further by Siebert *et al.* [1973] with a view to commercial applications.

Several investigations of fatigue behaviour are relevant to this study since transverse cracking may be induced by cyclic loading and it is also a common form of fatigue damage in glass fibre composites. Broutman [1964] and McGarry & Willner [1968] have studied fatigue behaviour at room temperature in orthotropic laminates using unmodified epoxy resins, and Owen *et al.* [1969] have studied fatigue failure in polyester resin-based composites. Increasing the toughness of epoxy resin [McGarry & Willner 1968] and the ductility of polyester resin [Owen & Rose 1970] has been shown to suppress resin cracking in cyclic loading situations; however, in the polyester composites, fibre debonding is unaffected and no significant improvement to fatigue life was detected with the flexibilised resin.

3. MATERIALS

Three laminates have been studied: a composite based on a 'standard' epoxy resin (No.10), one with the resin modified by the addition of a flexibiliser (No.15) and a third containing an elastomeric toughening agent (No.16). Details of these materials are given in Table 1.

The laminates comprised three plies, the inner ply being twice the thickness of outer plies and aligned at right angles to them. They were prepared by filament winding onto a flat rectangular mandrel. Entrapped air was removed by boiling off a volatile solvent (acetone or methyl chloride) from the resin under vacuum and then heating the laminate, with an electrical resistance element incorporated in the mandrel, until the resin was sufficiently fluid for the remaining bubbles to escape. The jig was then placed in an oven for the cure cycle. Test specimens of the resin were cast in open, polytetrafluoroethylene coated moulds and cured with the laminate.

4. TEST METHODS

The form and dimensions of the test specimens are shown in Figures 2 to 4. Test specimens were machined from the laminates with the fibres in the outer ply parallel to the specimen axis.

Tensile testing was carried out on a 4.45 kN Instron machine. Clamp type grips with upper and lower universal joints were used to ensure specimen alignment in the loading direction, and a thrust bearing was installed between the load cell and the upper grip to provide angular alignment of the grips in a plane perpendicular to the load. For short term tests (*e.g.* modulus determination), a strain rate of 10^{-2} min^{-1} was

used and the strain was monitored with an Instron strain gauge extensometer with a 50.8 mm gauge length. Elevated temperature tests were carried out in air in an Instron environmental chamber with a long-term temperature stability of ± 0.6°C.

Transverse cracking was studied under two testing procedures:

(1) Progressive Tensile Loading

The specimen was loaded to a certain stress; the modulus was then monitored, unloaded and inspected for cracks, reloaded to a higher stress and the process repeated to specimen failure. This test procedure gives an indication of the stress dependence of the cracking and also the effect of the cracking on the stiffness of the laminate.

(2) Cyclic Loading

To obtain information on cyclic loading behaviour, the specimen was cycled by loading to a constant maximum stress and then unloading with periodic modulus determination and inspection for cracks.

An estimate of the interply shear strength of the composite was obtained by a short beam bend test. The material was assumed to be homogeneous to simplify calculation of the strength.

The double torsion technique [Outwater & Gerry 1966] was used to obtain an estimate of the resin fracture toughness and the effect of stress range (load-unload) on the cycle-dependent crack propagation rate of the resins.

Although we are concerned principally with an application that has a service temperature of about 70°C, three test temperatures (room temperature (RT), 75°C and 100°C) were employed to give some insight into the influence of temperature on the materials under study.

5. RESULTS

5.1 Static Properties

The mechanical properties of the resins are listed in Table 2. An estimate of the glass transition temperature range can be obtained from the temperature dependence of the modulus (Figure 5). At 100°C, the unmodified resin has just entered the transition range, whereas the modified resins are about midway through the transition. The different temperature sensitivity is reflected in the higher elongation to fracture and lower tensile strength of the modified resins at 100°C. At 75°C, the modified resins are just at the lower end of the transition range and the differences are less pronounced.

The effect of temperature on the properties of the laminates is shown in Table 3. While the resin was in the glassy state, the strength and modulus were relatively insensitive to temperature, but in the transition range the laminate modulus decreased. The shear strength of the unmodified system was much higher than the modified systems with the flexibilised system showing the greatest decrease at high temperature.

Obvious cracking could not be detected by ear or by visual inspection in the flexibilised system at 100°C or in the toughened (opaque) system at 75 or 100°C. In these cases, although the stress-strain curve was non-linear in some tests, a definite 'knee' was not formed. Where a knee did occur, Table 3 shows that the strain involved was about the same for all resin systems, in accordance with the similarity of resin fracture strains (Table 2), and the strain to cause cracking increased progressively with temperature, reflecting the improved resin ductility.

5.2 Progressive Tensile Loading

The relationship between stress level and crack spacing found in the unmodified system at room temperature is shown in Figure 6. It can be seen that the spacing approached a limiting distance of about 1 mm. The final average crack spacings (determined by visual inspection or subsequent microscopical observation) in all systems are shown in Figure 7.

The concomitant changes in modulus for the unmodified system are also depicted in Figure 6. To simplify comparison of the various systems, the relative modulus at 600 MPa (the initial modulus (E_1) divided by the modulus determined by stressing to 600 MPa) is plotted against temperature (Figure 8). The modulus is reduced by 10 to 20 per cent except at temperatures where the resin is in the rubbery state.

The macroscopic appearance of the cracks in the unmodified system can be seen in Figure 9. At room temperature, the cracks proceeded rapidly across the ply, whereas at 75 and 100°C the growth rate was progressively slower. The opaque areas associated with some of the cracks near the edge of the specimen (and at the shoulders) are regions where the interply bond has failed.

A typical photomicrograph of the cracks in the unmodified system is given in Figure 10. In general, a crack proceeded more or less directly across the transverse ply, through the resin and around the fibres, but occasionally cracks were found at right angles to those within the ply.

The cracks often passed through voids, if they were present, but no evidence was found for resin-rich areas being preferred sites for cracks.

Scanning electron micrographs showing the surface of the crack in the unmodified system, exposed after separating the plies at room temperature, are presented in Figure 11. This figure shows that the crack ran through the matrix and around the fibres, sometimes apparently along the fibre/matrix interface and sometimes a short distance from it. It was difficult to detect any significant difference in crack path between the three systems, although the toughened system seemed to show more cracking through the resin.

5.3 Cyclic Loading

The cyclic crack growth rates observed in the resins at room temperature are plotted against the load (expressed as ΔG, the range of crack extension force) in Figure 12. From Table 2 it will be seen that the resistance to cycle-dependent crack growth increases with resin toughness.

The effect of cyclic loading on transverse cracking in the laminate composed of the unmodified resin is summarised in Figure 13. Each curve represents the increase in crack density in the transverse ply of a single specimen during cyclic loading. When the stress level is above the knee of the stress-strain curve, most of the cracking occurs in the first 100 cycles. The mean crack spacings after 1000 cycles in the unmodified and flexibilised systems are compared in Table 4. In the unmodified system, it appears that the susceptibility to cracking by cyclic loading is determined principally by the stress level and that the temperature has little effect, whereas in the flexibilised system, the cracking is more sensitive to temperature.

The change in modulus is influenced by the temperature. Table 5 shows the situation after 100 and 1000 cycles. Interpretation of these data is complicated by the scatter of results. The higher stresses do not consistently produce the greater reduction in modulus and no resin appears to give a uniformly better performance. The reduction in modulus, however, is generally alleviated by an increase in temperature.

The fatigue lives of the specimens used in these tests are plotted in Figure 14. The limited data indicate that, at high stress levels, the presence of the elastomer reduces the fatigue life.

At 100°C the macroscopic appearance of the cracks was influenced by the stress level(Figure 15). Cycling below the knee of the stress-strain

curve resulted in sharp and well-defined cracks, whereas cycling above the knee resulted in diffuse, less well-defined cracks, but even these were more regular than those formed during progressive tensile loading. Presumably, this reflects an influence of cycle-dependent crack growth on morphology.

Representative optical and electron optical photomicrographs of the cracks formed during cyclic loading are shown in Figures 16 and 17. The cracks appear to be generally similar to those formed on progressive tensile loading.

6. DISCUSSION

Initially, we shall discuss the phenomenon of transverse cracking in general terms in an attempt to identify the important parameters. We will then examine the effectiveness of the various resin systems.

When an orthogonal bi-directional laminate, such as was investigated in this study, is stressed along one of the material axes, the strain increases linearly with the stress until the failure strain of the weakest section of the transverse ply is reached. The elastic modulus of the laminate up to this stage is given by

$$E_1 = E_l \cdot a_l + E_t a_t \quad , \qquad (1)$$

where E_1 = primary modulus, E = ply modulus

a = area fraction of ply, l = longitudinal ply, and

t = transverse ply.

The load carried by the transverse ply is obviously zero at the fracture and the total load must be carried by the intact longitudinal plies. The stress will be transferred from the longitudinal plies by shear stresses and, as shown in Figure 18, the stress in the transverse ply will build up over a short distance (termed the stress transfer length, S) and will approach the pre-fracture level. The excess load in the intact plies will decrease to zero over the same distance. Depending on the test conditions (*i.e.* whether the testing machine is hard or soft), the failure of the ply will cause a small drop in load and/or a slight increase in strain in the test piece. Further straining takes place at reduced apparent modulus because the actual stress in the longitudinal plies around the fracture is higher than the apparent stress.

As mentioned above, the weakest section of the transverse ply will fail first but, in view of the numerous stress concentrators present

(*i.e.* the fibres), the strength of the transverse ply would be expected to be relatively uniform on a macroscopic scale, although there must be some small strength variation. Thus, after the first failure very little additional load would be supported by that ply and the apparent modulus would approach

$$E_2 = E_1 \cdot a_1 \quad , \tag{2}$$

where E_2 = secondary modulus, and (neglecting the small perturbation at the crack event) a linear stress-strain relationship would result. Typically, the transverse modulus of a unidirectional glass-fibre laminate is about 20-30 per cent of the longitudinal modulus, thus the primary and secondary modulus data shown in Table 3 are consistent with the above argument. If a laminate is unloaded from some stress σ_1 and strain ε_1 above the knee, then the modulus shown on reloading to σ_1, ε_1 will be some value between E_1 and E_2.

To recapitulate, the primary modulus is determined by the modulus of both longitudinal and transverse plies in proportion to their area fractions. The knee of the stress-strain curve is determined by the failure strain of the transverse ply (essentially the product of the resin failure strain and the stress concentration factor in the ply). The secondary modulus is determined principally by the modulus of the intact ply and its area fraction.

Where a definite knee is not formed in the stress-strain curve, two possibilities must be considered:

(1) When a negligible portion of the load is supported by the transverse layer (*e.g.* when the resin is above its glass-transition point), a linear stress-strain relationship will apply even though the transverse ply may be cracking.

(2) Under conditions of slow crack growth, where continual increase in stress is necessary to propagate the cracks, the knee will occur over a range of stresses and the stress-strain relationship will be non-linear.

Both of these conditions were observed in our tests.

We will now consider the relationship between the crack spacing and the applied stress. After the first crack, the transverse ply can be regarded as being made up of two regions. Immediately each side of the crack, for length S, the strain will be significantly reduced (as explained

previously). In the remainder of the ply, the strain will be reduced slightly below the previous level. Each subsequent crack gives rise to a similar pair of regions (Figure 17). Assuming, as a first approximation, that the reduction in strain occurring in the region farthest from the crack is inversely proportional to the length of those regions, we have

$$\eta = \frac{k}{L - 2NS} \quad , \tag{3}$$

where k = a constant which includes effects of specimen geometry,

L = gauge length, and N = number of cracks in gauge length.

The stress σ necessary to bring the strain in these regions back to the fracture strain is then

$$\sigma = E_{\eta} = \frac{kE}{L - 2NS} \tag{4}$$

and, on rearranging,

$$N = \frac{L}{2S} - \frac{kE}{2S} \frac{1}{\sigma} \quad . \tag{5}$$

If N is plotted against $\frac{1}{\sigma}$, a straight line is obtained (Figure 19); the intercept gives S = 0.4 mm and kE can be determined from the slope. When these values are applied to Equation (4), the resultant curve (Figure 6) depicts the crack spacing approaching a minimum value of about 1.0 mm. As shown in Figure 18 the ultimate mean crack spacing will lie somewhere between 2S and S, a reasonable estimate being 1.55 (about 0.6 mm). The discrepancy between the observed and estimated spacings is easily accounted for by the small amount of delamination at the crack site (see Figure 9) which must be present because the crack opens and closes during loading and unloading.

The transfer length is related to material properties. The distance over which the load builds up in the transverse ply depends on the shear forces at the upper and lower ply interfaces. The maximum shear force is limited by the shear strength of the interface and the stress in the ply will reach its fracture stress at the transfer length S.

Hence, with reference to Figure 18, we have

$$dw\sigma_{tf} = 2Sw\tau \quad ,$$

where d = transverse ply thickness, w = ply width,

σ_{tf} = fracture stress of transverse ply, and

τ = interply shear strength;

therefore

$$S = \frac{d\sigma_{tf}}{2\tau} \quad . \tag{6}$$

For the unmodified system, we have at RT, d = 0.98 mm and τ = 54 MPa, and $\sigma_{tf} = \varepsilon_b E_T$, where ε_b = 0.0055 is the strain at first break and the modulus E_t = 10.2 GPa is estimated from Equations (1) and (2). These figures give a value for S of 0.5 mm which is in very good agreement with both the previous estimate and the observed value.

The above analyses have defined in semi-quantitative terms some of the steps to be taken to increase the ultimate mean crack spacing (1.55), *i.e.* increasing the transverse ply thickness and the transverse ply fracture strength will decrease the interply shear strength, whereas to decrease the number of cracks at a given stress, both the elastic modulus of the laminate and the stress transfer length (S) should be increased.

We shall now turn our attention to the effectiveness of the various resin systems on the cracking behaviour of the laminates.

The experimental measurements of the ultimate crack spacings in Figure 7, indicate somewhat unexpectedly, that the unmodified system generally had higher values than the modified systems. Analysis of the crack spacing in terms of Equation (6) is, however, only appropriate where the cracking was abrupt and completely transversed the ply. Macroscopic and microscopic inspection (*e.g.* Figure 9 and 16) indicates that these conditions were only met at RT and 75°C for the unmodified and flexibilised systems and, perhaps, at RT for the toughened system. The spacings estimated *via* Equation (6) for these conditions are plotted in Figure 7. Agreement with the observed spacings is rather better with the unmodified system than with the modified systems but, considering the uncertainties involved in estimating the shear strength and the elastic modulus of the transverse ply, the overall agreement is reasonable.

The progressive loading experiments also show that, in conformity with the ideas behind the development of Equations (1) and (2), the decrease in stiffness due to cracking is not greatly dependent on the

resin system (Figure 8); mainly it depends on whether the resin is in the glassy or rubbery state.

One problem that is still unresolved by the progressive loading experiments is whether the failure stress of the transverse ply is determined by the strength and/or strain of the resin or by the properties of the interface between the glass and the resin. Scanning electron microscopy (*e.g.* Figures 11 and 17) shows that, in all systems, the crack often seems to travel along the interface, but no obvious differences between the resin systems were noted.

Identification of the influence of resin properties on cracking under cyclic loading has also proved to be elusive. Figure 13 and Table 4 show that, in the systems where the cracking can be visually monitored, the susceptibility to cracking by cyclic loading is principally determined by the stress level; they also indicate that neither the resin system nor the temperature has much effect.

Although increased temperature does alleviate the decrease in stiffness on cyclic loading (Table 5) this is due, in part, to the decreased effectiveness of the resin matrix at higher temperatures and the results do not reveal any systematic effect of resin properties. Once again, such behaviour is consistent with the principles behind Equation (2), that once the ply is fully cracked across a section its contribution to the stiffness of the laminate is largely lost.

The superior resistance to cycle-dependent crack propagation of the toughened system (Figure 12) is not reflected in the cyclic loading tests on the laminates; presumably this is because of the over-riding influence of stress and the strain concentration effect of the fibres. As indicated in Figure 14, the cyclic loading tests at those levels below which immediate cracking does not occur have not been completed.

7. CONCLUSIONS

This work has identified the main phenomenological aspects of transverse cracking and has enabled some conclusions to be drawn regarding the influence of the resin system on cracking behaviour.

When the resin is in the glassy state, simply increasing resin toughness is not effective in suppressing cracking at high stress levels, although the cracks induced by cyclic loading at low stress levels should be inhibited. With brittle resins, the ultimate crack spacing and the relationship between stress and crack spacing can be explained

in terms of shear stress transfer from the longitudinal plies. If the toughness of the resin is sufficient to allow slow crack growth, a more closely spaced array of irregular cracks is formed. The elastic modulus of the laminate is lowered by transverse cracking, but the modulus in both the cracked or uncracked state is not greatly affected by the modulus of the resin.

Even the high ductility of resins in the rubbery state is not sufficient to prevent transverse cracking although, because of the very low elastic modulus of the resin, such cracking is not accompanied by large reductions in the stiffness of the laminate.

Microscopic examination indicates that the cracking occurs both in the resin and at (or very close to) the resin/glass fibre interface. It was not possible to determine the region in which the crack is initiated.

8. ACKNOWLEDGEMENTS

We wish to thank Messrs A.M. Spencer and H.H. Muller for fabricating the laminates, and Mr. T. Davidson for carrying out the fibre content determinations.

9. REFERENCES

Broutman, L.J. [1964] - 19th Ann. Tech. and Management Conf., Chicago, SPI Reinforced Plastics Div., Section 1-A. The Society of the Plastics Industry Inc.,New York.

Epstein, G. & Bandaruk, W. [1964] - 19th Ann. Tech. and Management Conf., Chicago, SPI Reinforced Plastics Div., Section 19-D. The Society of the Plastics Industry Inc.,New York.

Kies, J.A. [1962] - NRL 5752.

Lavengood, R.E. & Ishai, O. [1971] - Polymer Eng. and Sci., 11(3)226.

McGarry & Willner, A.M. [1968] - 23rd Ann. Tech. Conf., Washington DC, SPI Reinforced Plastics/Composites Div., Section 14-B. The Society of the Plastics Industry Inc.,New York.

Outwater, J.O. & Gerry, D.J. [1966] - AD 640 848.

Owen, M.J. & Rose, R.G. [1970] - Mod. Plastics, 47(11)130

Owen, M.J., Smith, T.R. & Dukes, R. [1969] - Plastics and Polymers 37(3)227.

Rawe, R.A. [1962] - Standards for filament-wound reinforced plastics , ASTM STP 327, p.248.

Schultz, J.C. [1963] - 18th Ann. Tech. and Management Conf., Chicago, SPI Reinforced Plastics Div., Sect 7-D. The Society of the Plastics Industry Inc., New York.

Siebert, A.R., Rowe, E.H., Riew, C.K. & Lipiec, J.M. [1973] - 28th Ann. Conf., Washington DC, SPI Reinforced Plastics/Composites Inst. Section 1-A. The Society of the Plastics Industry Inc., New York.

10. NOTATION

- E_1 - primary elastic modulus of composite
- E_2 - secondary elastic modulus of composite
- E_l - elastic modulus of longitudinal ply
- E_t - elastic modulus of transverse ply
- L - gauge length
- N - number of cracks in gauge length
- S - stress transfer length
- a_l - area fraction of longitudinal ply
- a_t - area fraction of transverse ply
- d - transverse ply thickness
- k - constant
- w - ply width
- ε - strain
- σ - stress
- σ_{tf} - fracture stress of transverse ply
- η - strain decrement due to crack
- τ - interply shear strength

TABLE 1

DETAILS OF MATERIALS

Material Code	Resin Composition (parts by weight)					Glass Fibre	
	Resin	Hardener	Accelerator	Flexibiliser	Elastomer	Type	Content
	Araldite LY556	HY906 (NMA*)	HY960 (DMP-30*)	Araldite CY-208	Hycar CTBN		
10	100	80	0.75	0	0	Owens-Corning S glass	58.0
	Araldite F		DY062 (BDMA*)				
15	80	80	1.5	20	0	Ferro Unistrand	60.8
16	100	80	1.5	0	18	"	61.0

Cure Cycle - 2 h, 100°C; 16 h, 150°C

* NMA - Nadic methyl anhydride DMP-30 - Tris (dimethylaminomethyl) - phenol

BDMA - Benzyldimethylamine

TABLE 2

PROPERTIES OF RESIN SYSTEMS

Resin Code	Hardness (Barcol No) RT	Fracture Toughness ($J\ m^{-2}$)			Ultimate Tensile Stress (MPa)			Elongation (%)		
		RT	75°C	100°C	RT	75°C	100°C	RT	75°C	100°C
10	33	99	418	n.d.	58.2	53.2	41.4	2.8	3.0	10.1
15	25	277	7770	n.d.	60.8	44.2	15.9	2.2	4.5	30.4
16	9	3150	n.d.	n.d.	58.8	32.7	12.1	3.9	4.6	26.7

n.d. - not determined, resin too ductile.

TABLE 3

MECHANICAL PROPERTIES OF LAMINATES

Material	Temp. (°C)	Ultimate Tensile Stress			Primary Modulus			Secondary Modulus			Strain to 1st Transverse crack			Interlaminar Shear Stress		
		Mean (MPa)	No. of Tests	c.v.† (%)	Mean (GPa)	No. of Tests	c.v. (%)	Mean (GPa)	No. of Tests	c.v. (%)	Mean	No. of Tests	c.v. (%)	Mean (MPa)	No. of Tests	c.v. (%)
10	RT	909	1	-	35.5	7	7.0	25.3	4	2.8	0.57	7	18.6	52	4	9.4
	75	778	1	-	30.8	4	6.5	25.8	3	8.6	0.80	3	9.3	51	5	12.6
	100	807	1	-	30.3	4	8.4	25.3	2	8.3	1.10	2	18.0	45	5	6.1
15	RT	788	1	-	30.0	5	8.1	22.3	3	6.6	0.41	4	8.4	41	6	6.6
	75	777	1	-	28.3	4	7.1	22.0	3	9.6	0.69	3	5.8	26	6	10.9
	100	721	1	-	23.1	4	7.7	n.d.			n.d.			20	6	14.9
16	RT	722	1	-	29.8	4	9.1	21.5	3	5.9	0.42	3	13.9	34	6	10.9
	75	676	1	-	28.2	4	17.2	n.d.			n.d.			34	6	4.8
	100	646	1	-	25.0	4	10.3	n.d.			n.d.			23	6	4.1

* n.d. - not detected † c.v. - coefficient of variation

TABLE 4

EFFECT OF STRESS AND TEMPERATURE ON

CRACKING UNDER CYCLIC LOADING

Material	Temp. (°C)	Crack Spacing after 1000 cycles		
		138 MPa (mm)	345 MPa (mm)	552 MPa (mm)
10	RT	3.63	1.37	1.08
	75	2.21	1.30	n.d.
	100	2.42	1.45	n.d.
15	RT	1.88	2.12	2.19
	75	1.37	1.30	1.63
	100	1.10	1.12	n.d.

n.d. - specimen failed before 1000 cycles

TABLE 5

EFFECT OF STRESS AND TEMPERATURE

ON THE REDUCTION OF STIFFNESS

DURING CYCLIC LOADING

Material	Temp. (°C)	Relative Modulus $\left(\frac{E_{cycle\ 100}}{E_{cycle\ 1}}\right)$		
		138 MPa	345 MPa	552 MPa
10	RT	0.96	0.85	0.80
	75	1.00	0.97	0.61
	100	1.00	0.96	n.d.
15	RT	0.81	0.83	0.86
	75	0.84	0.84	0.92
	100	1.00	1.00	
16	RT	0.86	0.94	0.84
	75	0.94	1.00	n.d.
	100	0.92	1.00	n.d.
		Relative Modulus $\left(\frac{E_{cycle\ 1000}}{E_{cycle\ 1}}\right)$		
		138 MPa	345 MPa	552 MPa
10	RT	0.89	0.78	0.80
	75	0.93	0.93	n.d.
	100	1.00	0.98	n.d.
15	RT	0.79	0.79	0.88
	75	0.89	0.84	0.92
	100	1.00	0.92	n.d.
16	RT	0.86	0.96	n.d.
	75	0.90	1.00	n.d.
	100	0.98	n.d.	n.d.

n.d. - specimen failed before observation

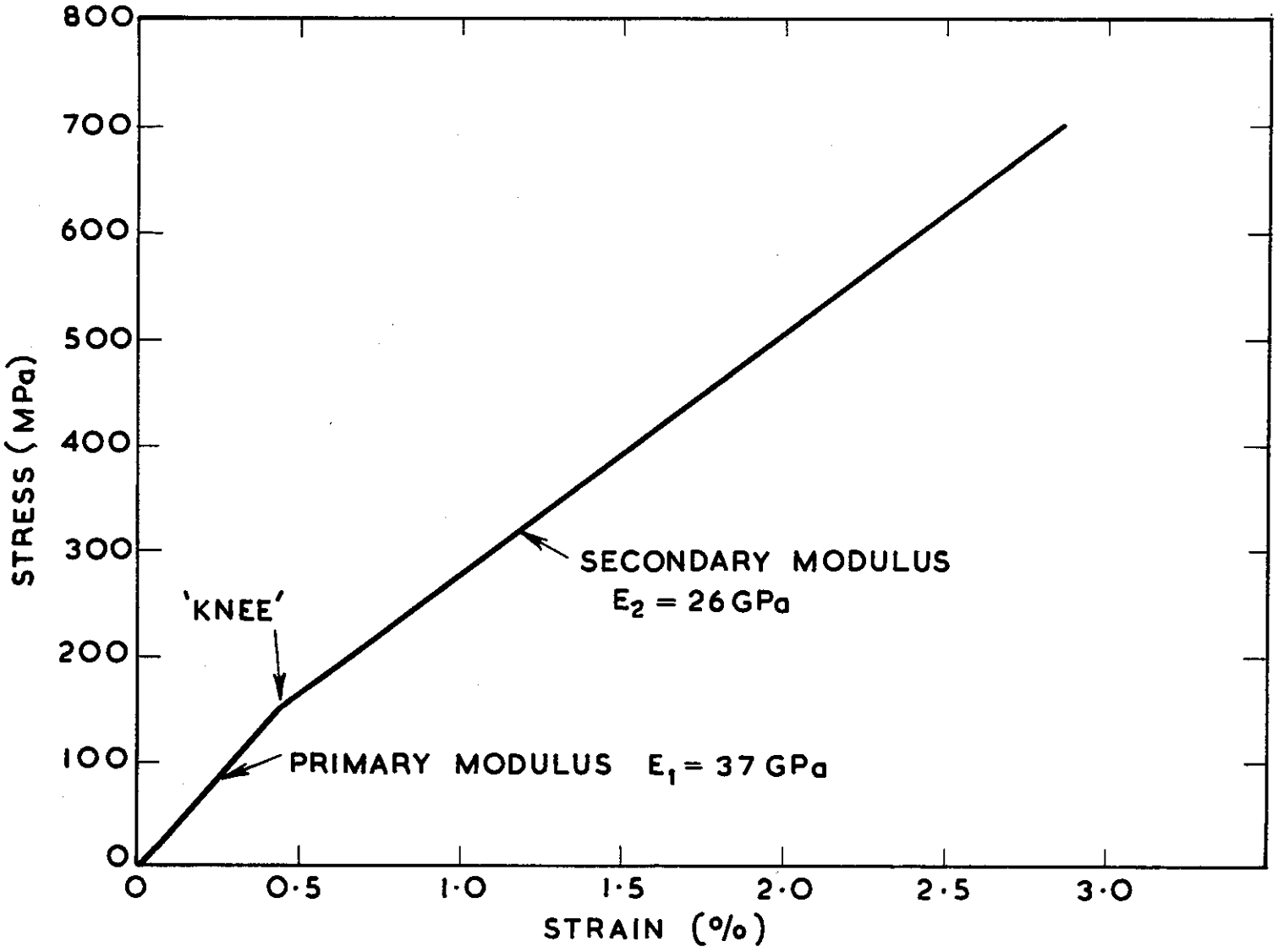

FIGURE 1. TYPICAL STRESS-STRAIN CURVE OF ORTHOTROPIC GLASS-FIBRE/EPOXY RESIN COMPOSITE WITH ONE OF THE FIBRE DIRECTIONS ALIGNED WITH THE TENSION AXIS

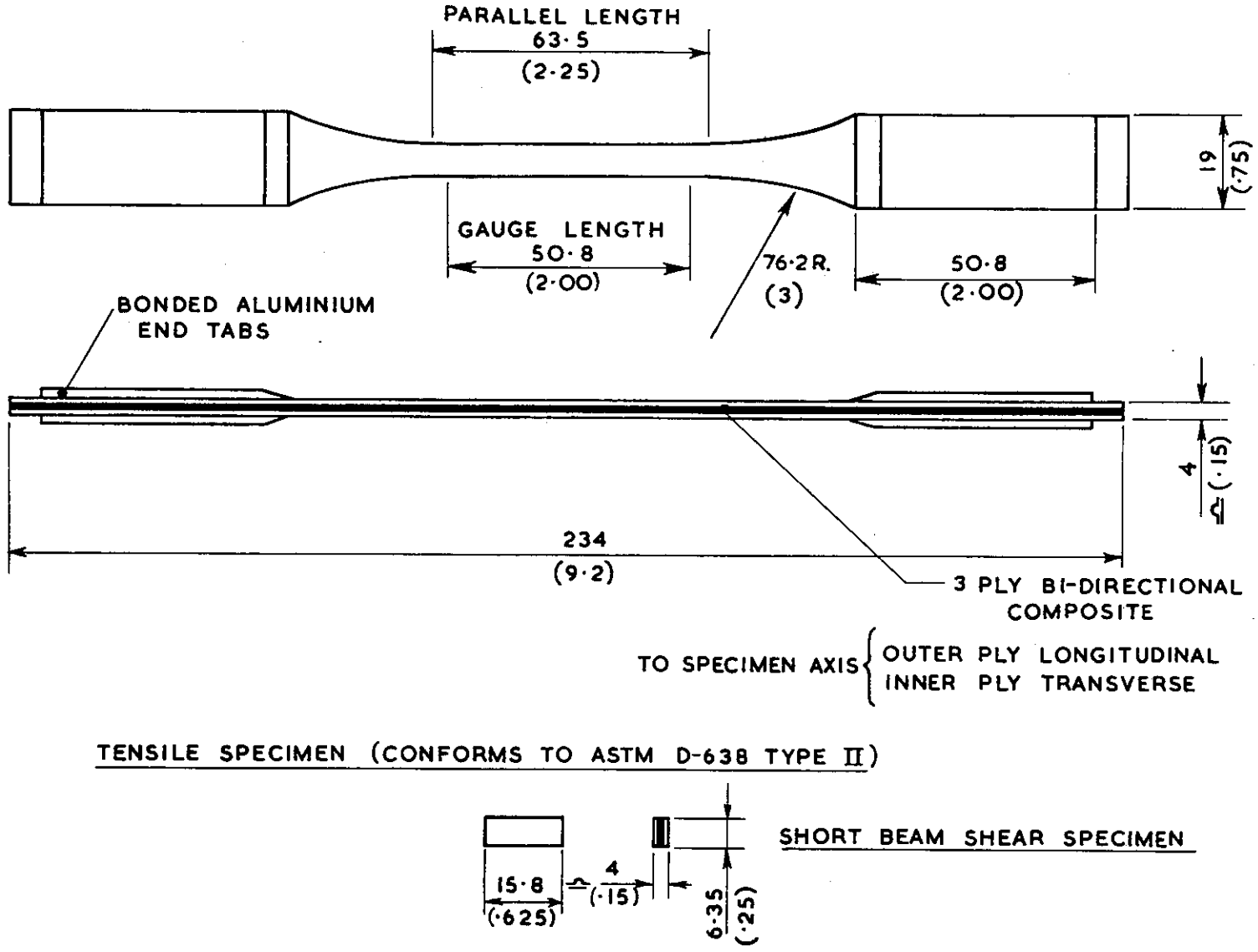

FIGURE 2. GLASS-FIBRE/RESIN TEST SPECIMENS, DIMENSIONS IN MILLIMETRES (AND ALSO IN INCHES)

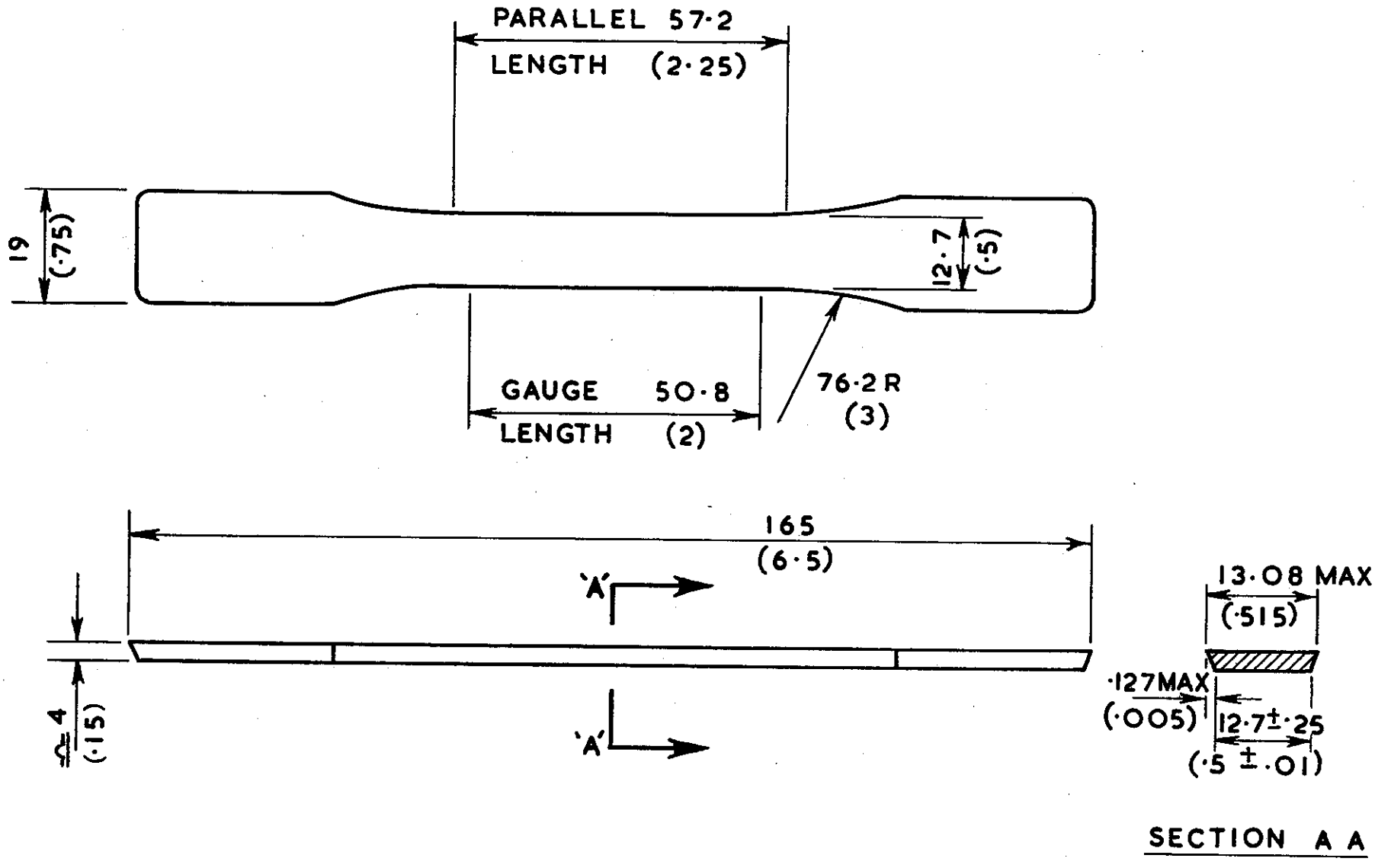

FIGURE 3. RESIN TENSILE TEST SPECIMEN, DERIVED FROM ASTM D-638 TYPE I.
DIMENSIONS IN MILLIMETRES (AND ALSO IN INCHES)

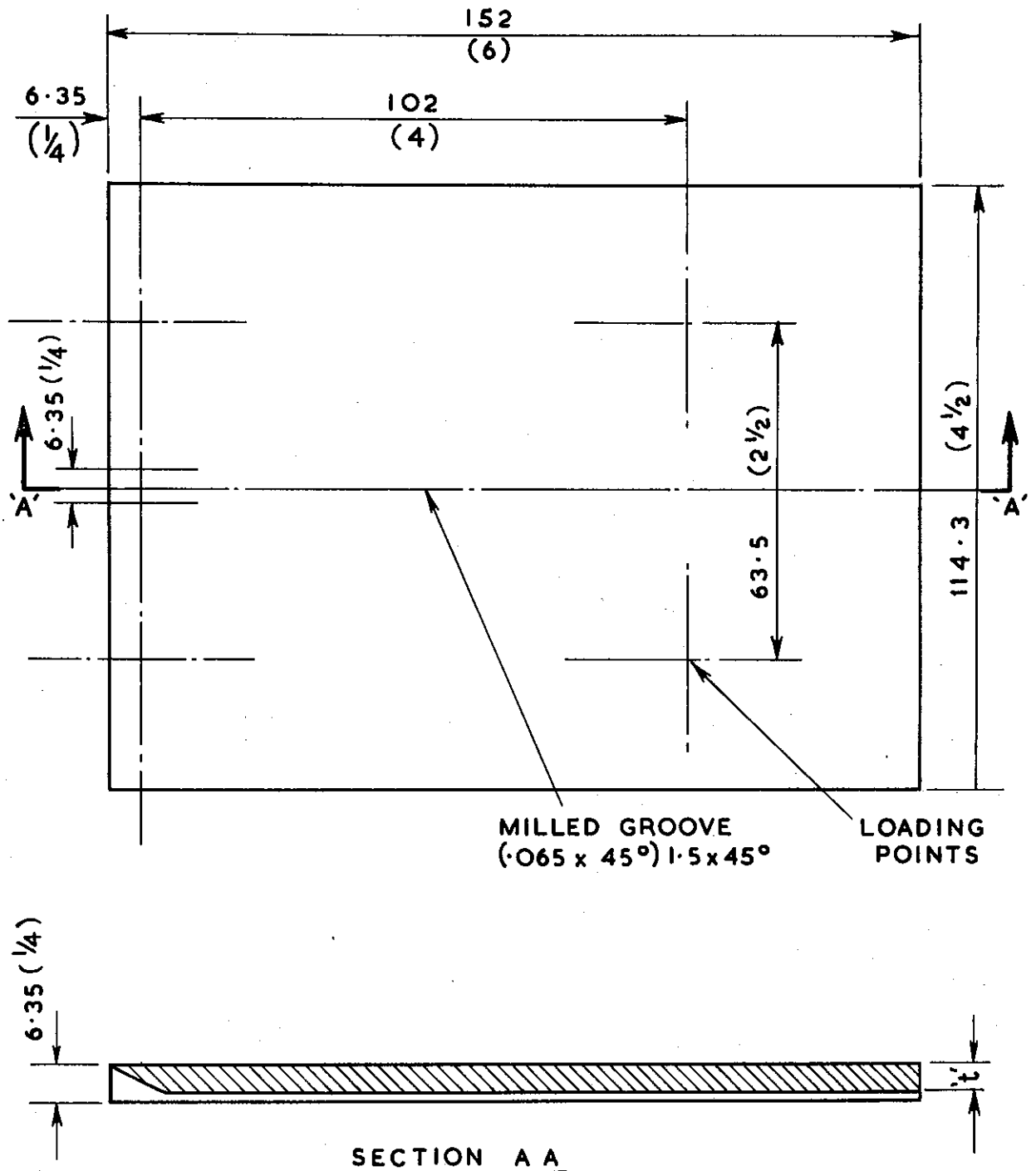

FIGURE 4. RESIN FRACTURE TOUGHNESS SPECIMEN, DIMENSIONS IN MILLIMETRES (AND ALSO IN INCHES)

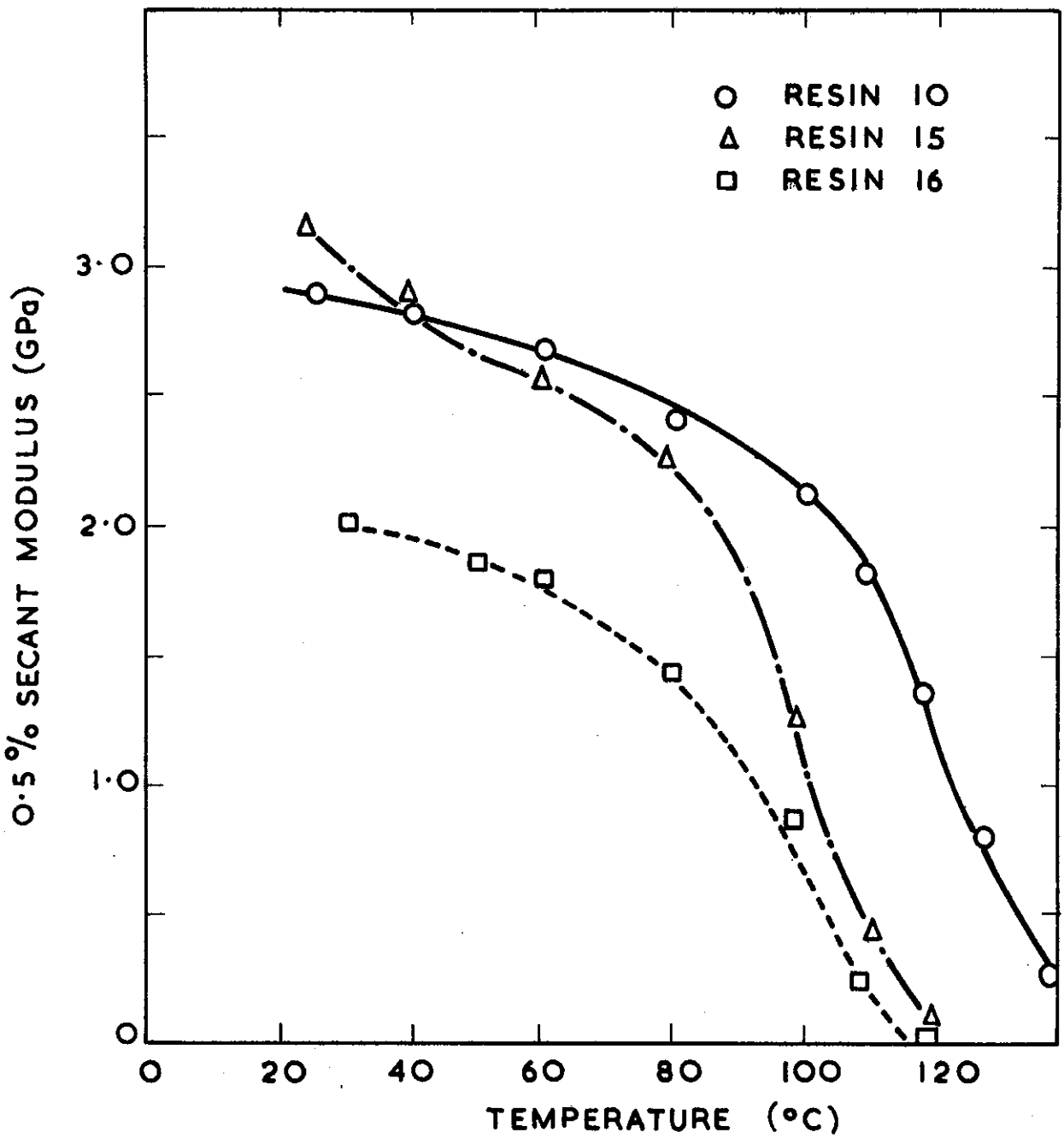

FIGURE 5. EFFECT OF TEMPERATURE ON THE ELASTIC MODULUS OF THE RESIN SYSTEMS

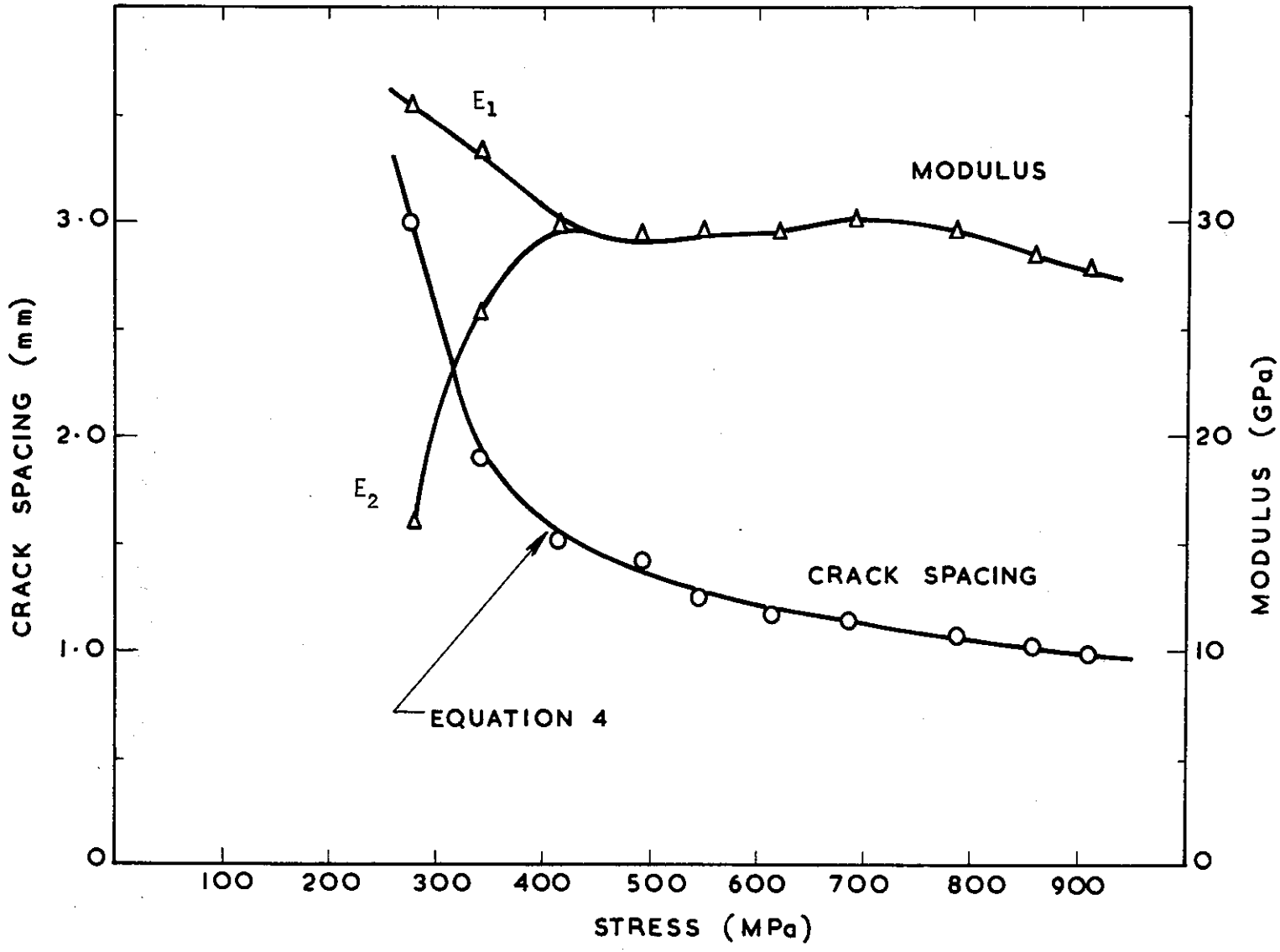

FIGURE 6. RELATIONSHIP BETWEEN STRESS LEVEL, MODULUS AND CRACK SPACING IN MATERIAL 10 AT ROOM TEMPERATURE

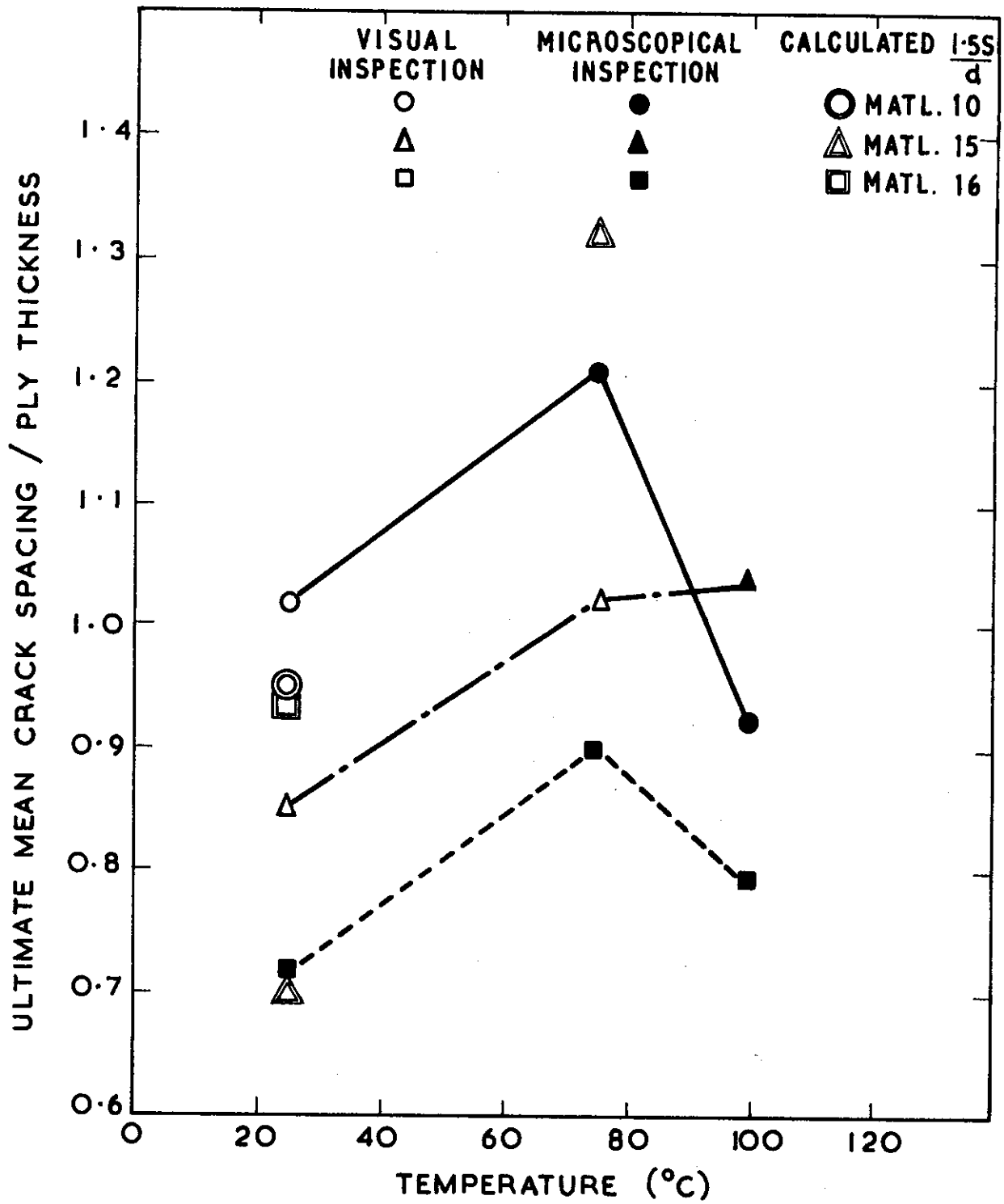

FIGURE 7. MINIMUM CRACK SPACINGS OBSERVED IN LAMINATES COMPARED WITH CALCULATED VALUES

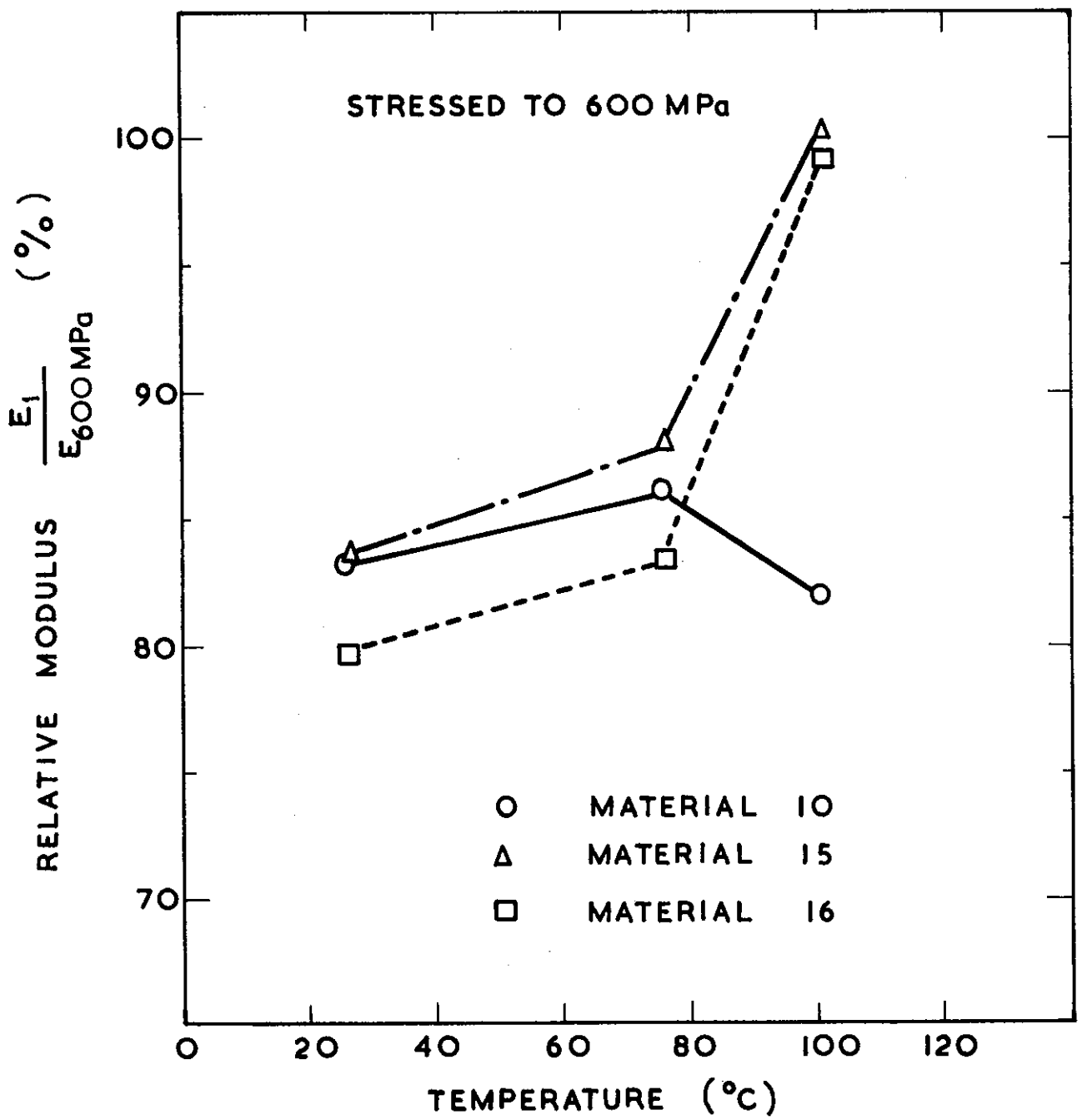

FIGURE 8. CHANGE IN MODULUS OF LAMINATES STRESSED TO 600 MPa

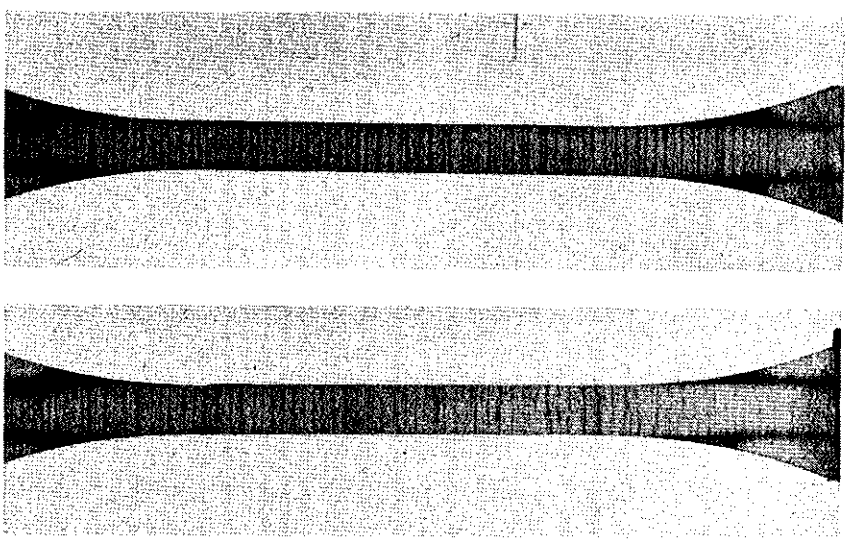

FIGURE 9. TRANSVERSE CRACKS IN MATERIAL 10. UPPER FORMED AT ROOM TEMPERATURE, LOWER FORMED AT 100°C (ACTUAL SIZE)

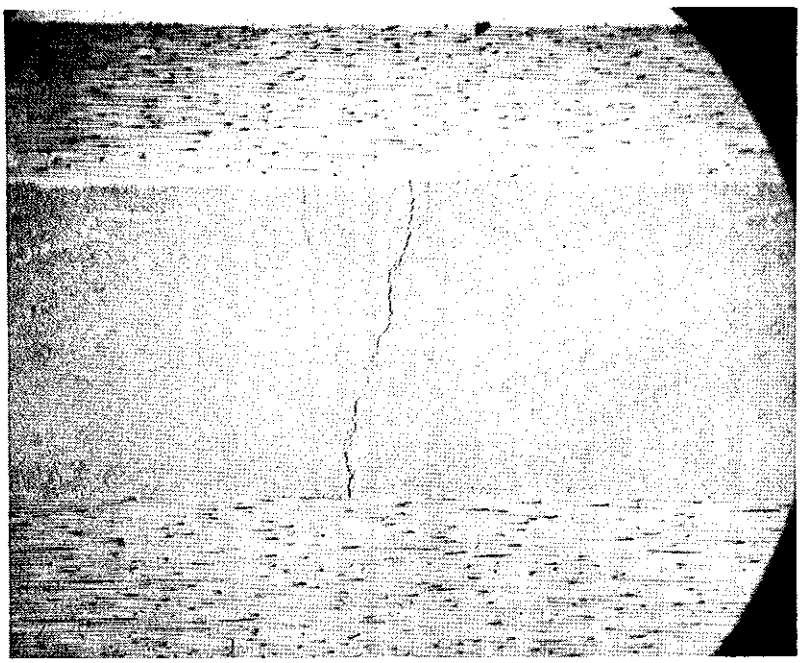

(a) 50×

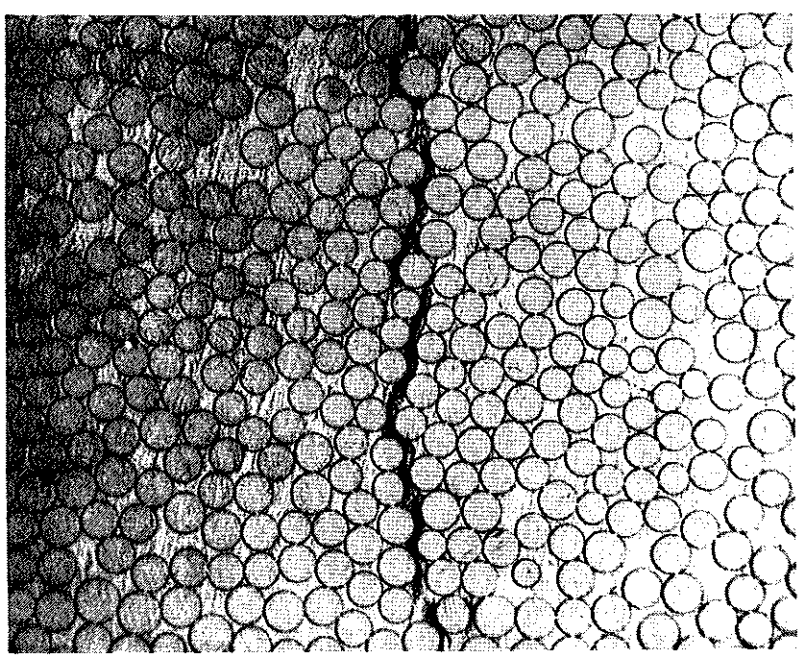

(b) 500×

FIGURE 10. TRANSVERSE CRACK IN MATERIAL 10 FORMED AT ROOM TEMPERATURE

(a) RT 540×

(b) 75°C 490×

(c) 100°C 490×

FIGURE 11. SCANNING ELECTRON MICROGRAPHS OF SURFACE OF TRANSVERSE CRACK IN MATERIAL 10

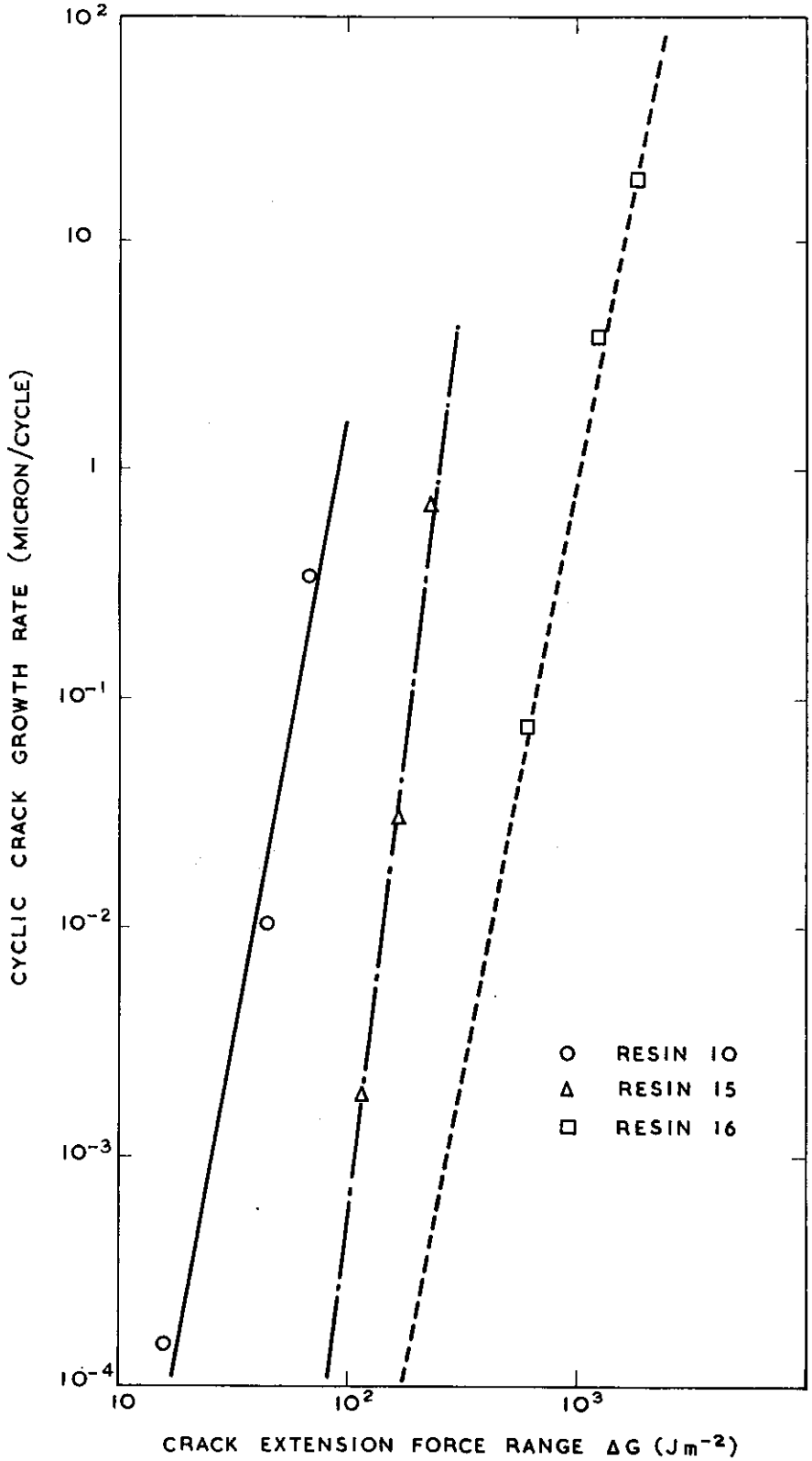

FIGURE 12. CYCLIC CRACK GROWTH RATE OF RESIN SYSTEMS AS A FUNCTION OF THE LOAD RANGE AT ROOM TEMPERATURE

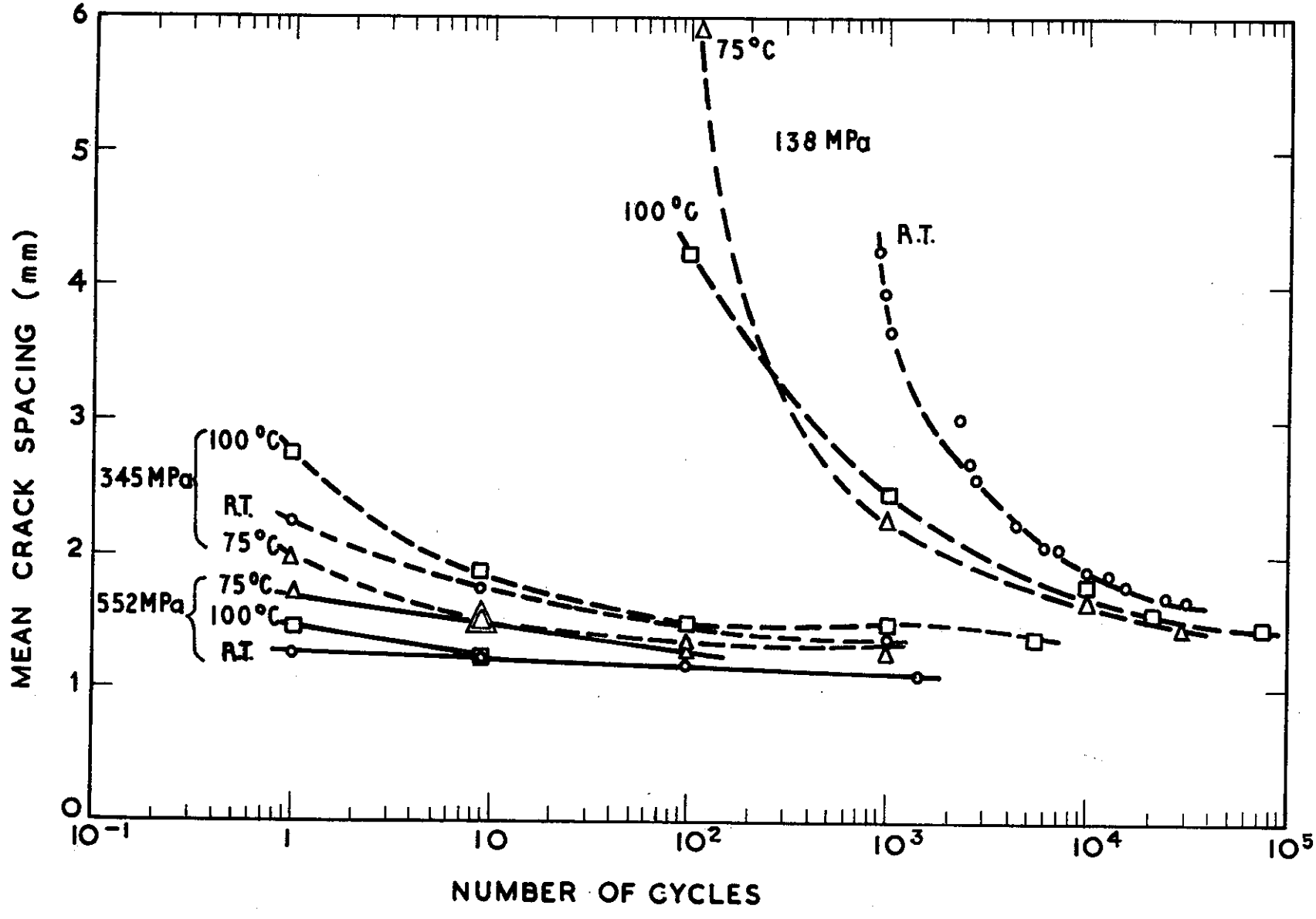

FIGURE 13. TRANSVERSE CRACKING INDUCED IN MATERIAL 10 BY CYCLIC STRESSING (LOAD-UNLOAD)

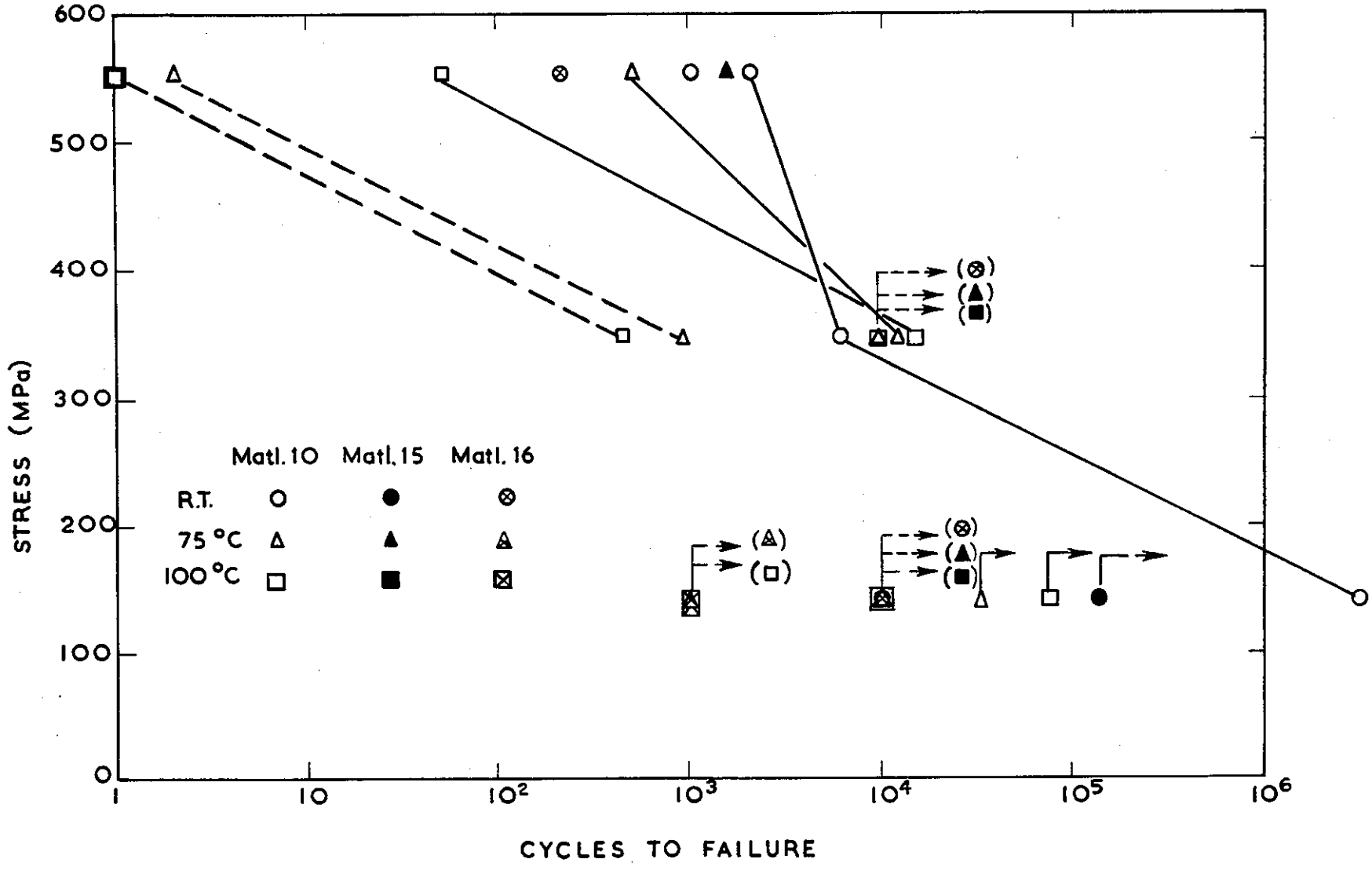

FIGURE 14. FATIGUE LIFE OF LAMINATES. NO FAILURES WERE RECORDED AT 138 MPa

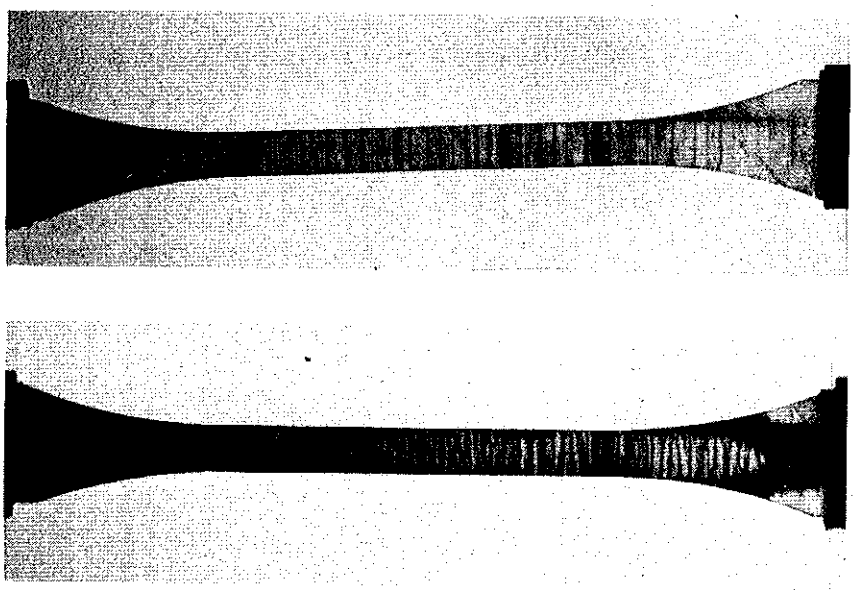

FIGURE 15. TRANSVERSE CRACKS FORMED BY CYCLIC LOADING IN MATERIAL 15 AT 100°C. UPPER - 10,000 CYCLES TO 138 MPa, LOWER - 10,000 CYCLES TO 345 MPa (ACTUAL SIZE)

(a) 50×

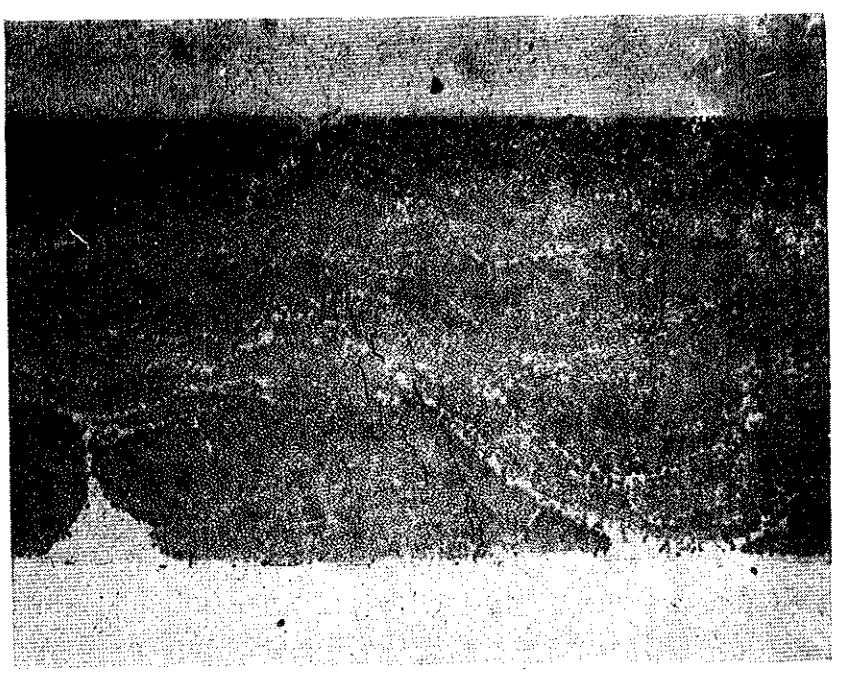

(b) 50×

FIGURE 16. TRANSVERSE CRACKS FORMED BY CYCLIC LOADING IN MATERIAL 10 AT 100°C; (a) - TO 345 MPa, (b) - TO 552 MPa

(a) 490×

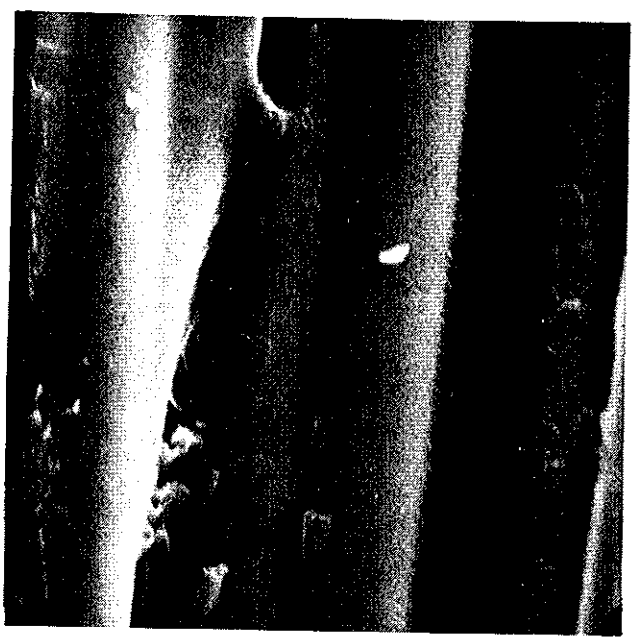

(b) 1660×

FIGURE 17. SCANNING ELECTRON MICROGRAPH OF SURFACE OF TRANSVERSE CRACK IN MATERIAL 10 FORMED BY CYCLIC LOADING TO 345 MPa AT 100°C

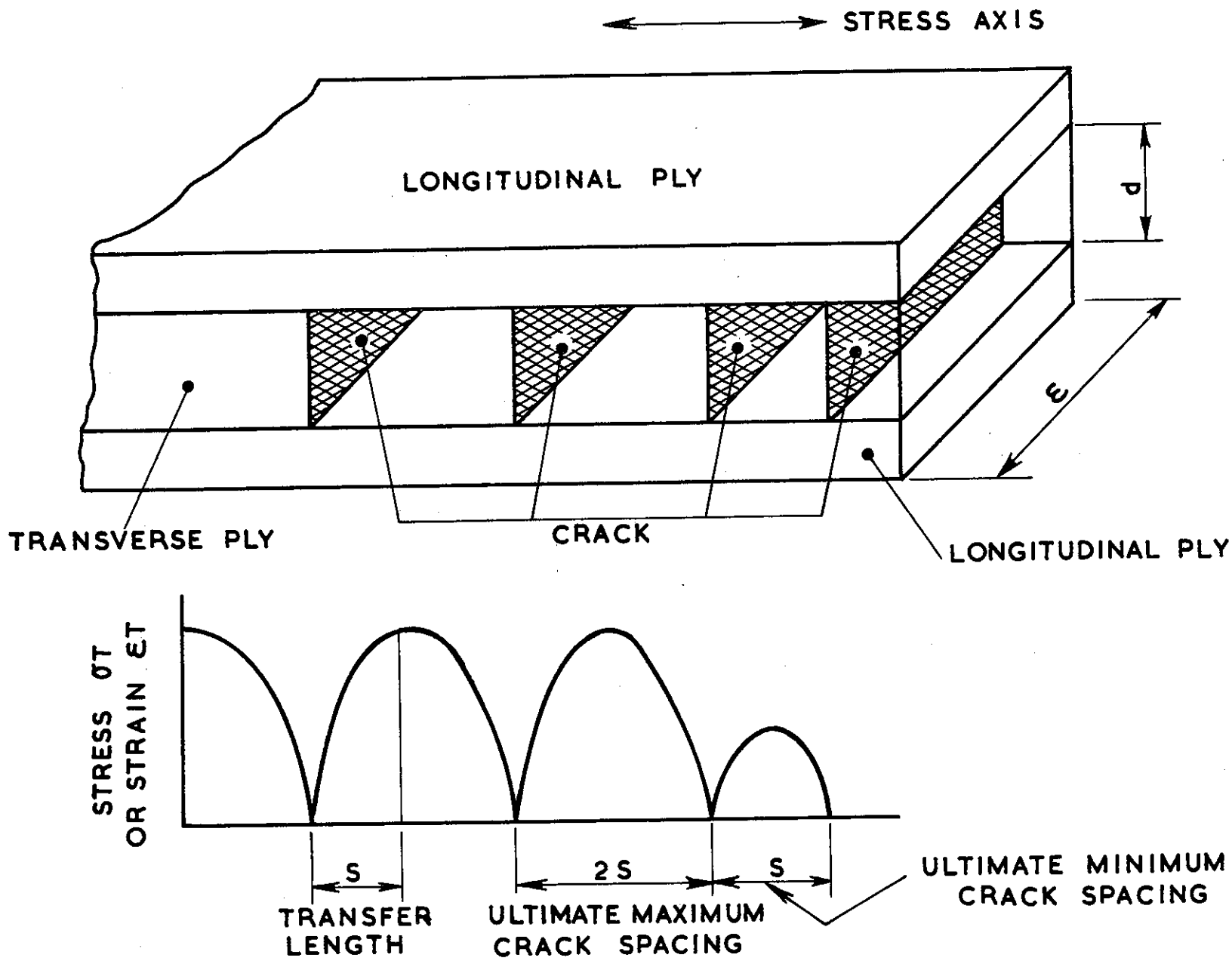

FIGURE 18. SCHEMATIC ILLUSTRATION OF TRANSVERSE CRACKING

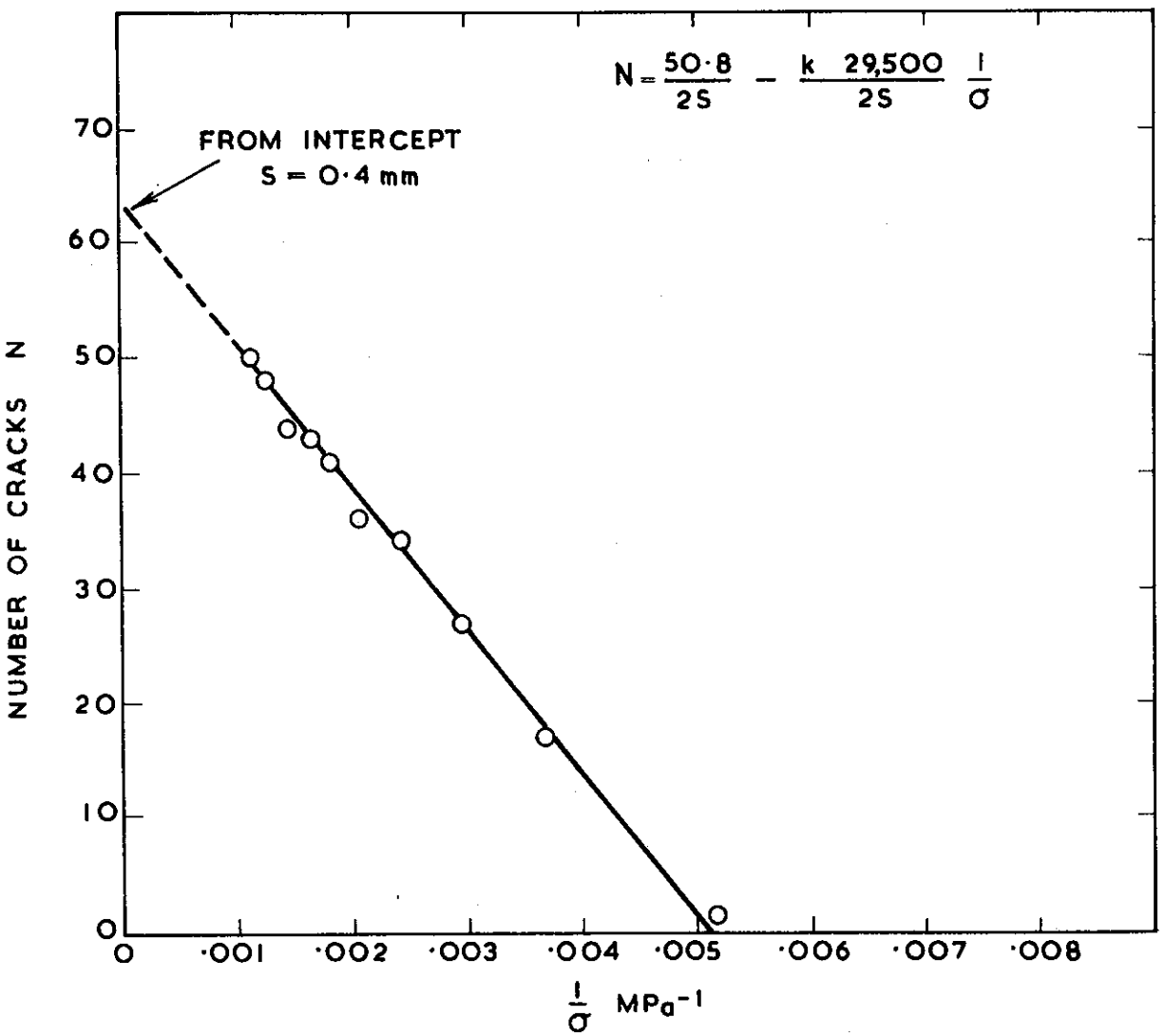

FIGURE 19. COMPARISON OF THEORETICALLY PREDICTED CRACK SPACINGS WITH THOSE OBSERVED IN MATERIAL 10 AT ROOM TEMPERATURE